

QCD transition at the physical point, and its scaling window from twisted mass Wilson fermions

Andrey Yu. Kotov^{a,b}, Maria Paola Lombardo^c, Anton Trunin^d

^aJuelich Supercomputing Centre, Forschungszentrum Juelich, D-52428 Juelich, Germany

^bBogoliubov Laboratory of Theoretical Physics, Joint Institute for Nuclear Research, Dubna, 141980 Russia

^cINFN, Sezione di Firenze, 50019 Sesto Fiorentino (FI), Italy

^dSamara National Research University, Samara, 443086 Russia

Abstract

We study the scaling properties of the finite temperature QCD phase transition, for light quark masses ranging from the heavy quark regime to their physical values. The lattice results are obtained in the fixed scale approach from simulations of $N_f = 2 + 1 + 1$ flavours of Wilson fermions at maximal twist. We identify an order parameter free from the linear contributions in mass due to additive renormalization and regular terms in the Equation of State, which proves useful for the assessment of the hypothesized universal behaviour. We find compatibility with the 3D $O(4)$ universality class for the physical pion mass and temperatures $120 \text{ MeV} \lesssim T \lesssim 300 \text{ MeV}$. We discuss violation of scaling at larger masses and a possible cross-over to mean field behaviour. The chiral extrapolation $T_0 = 134^{+6}_{-4} \text{ MeV}$ of the pseudocritical temperature is robust against predictions of different universality classes and consistent with its estimate from the $O(4)$ Equation of State for the physical pion mass.

1. Introduction

The appearance of pseudo-Goldstone bosons in the spectrum signals the spontaneous breaking of chiral symmetry of strong interactions. It is well known that chiral symmetry is restored at high temperatures, and imprinting of this phenomenon for physical masses is visible in the behaviour of the order parameters and in the spectrum. If the symmetry restoring transition is continuous, the link between the genuine critical behaviour in the chiral limit and the observations at finite masses is made transparent by the universal Equation of State (EoS). This is true only within a limited region around criticality – the scaling window.

Despite substantial progress [1, 2], the nature of the continuum limit and the extent of its scaling window are still open issues. Chiral and axial symmetries play a pivotal role here: in this study we make use, as in our previous work, of Wilson fermions at maximal twist [3–7], a lattice formulation with good chiral properties and an alternative to the more used staggered fermions.

The global symmetry of the QCD Lagrangian $U(n)_L \times U(n)_R \cong SU(n) \times SU(n) \times U(1)_V \times U(1)_A$, valid at classical level, is broken by topological quantum fluctuations. In the limit of an infinite strange mass there are at least two possible scenarios for the high temperature transition depending on the fate of the axial symmetry [8–10]: if the axial symmetry breaking is not much sensitive to the chiral restoration, the breaking pattern is $SU(2)_L \times SU(2)_R \rightarrow SU(2)_V$. Due to the associate diverging

correlation length, the theory is effectively 3D, in the universality class of the classical four-component Heisenberg antiferromagnet: $O(4) \rightarrow O(3)$ [8]. If instead axial symmetry is correlated with chiral symmetry, the relevant breaking pattern would be $U(2)_L \times U(2)_R \rightarrow U(2)_V$, hinting either at a first or at a second order transition with different exponents [10].

We are interested in properties of the transition for physical values of the strange quark mass m_s . If the two flavor transition is of first order, we are likely dealing with a first order transition for any m_s . Alternatively, if the $m_s = 0$ first order transition ends at $m_s = m_{\text{crit}}^s$, m_s merely renormalizes the coefficients of the effective action for $m_s > m_{\text{crit}}^s$ [8, 9], without altering the critical behaviour. In this case one conventionally assumes that there is a line of second order transition $T_c(m_l = 0, m_s) > T_c(m_l = 0, m_s)$ for $m_l = 0, \infty > m_s > m_{\text{crit}}^s$. Away from the true critical point dimensional reduction may fail, resulting in a 4D theory and a mean field behaviour. The extent of the scaling window and the threshold of dimension reduction are non-universal features, which should be investigated by ab-initio methods.

These important issues are addressed by model studies [11–14], phenomenological analysis [15–17], Functional Renormalization Group [18–21], and mostly on the lattice [3, 4, 22–29]. Consistency with $O(4)$ scaling has been reported in lattice studies of the theory with two light and strange flavors, at low pion mass [1, 30], once different sources of scaling violations are taken into account. The same study finds a critical temperature in the chiral limit $T_0 = 132^{+3}_{-6} \text{ MeV}$. Consistency with $O(4)$ scaling was found also by earlier studies with Wilson fermions, see e.g. [7, 31, 32]. Concerning axial symmetry, the current understanding is that it seems to be effectively restored above T_c [22, 27, 33–45], but there is no consensus on the restoration

Email addresses: a.kotov@fz-juelich.de (Andrey Yu. Kotov), lombardo@fi.infn.it (Maria Paola Lombardo), amtrnn@gmail.com (Anton Trunin)

temperature. On the analytic side, a 4D analysis [46] reported scaling only for very light pion masses, $m_\pi < 1$ MeV, and an apparent scaling for larger masses. The same study underscores the lack of dimensional reduction as a potential source of scaling violations. A recent work [21] confirms these findings, suggesting that pion masses as light as 30 MeV are needed to reach the scaling window in QCD, with a consistent extrapolation to $T_0 \simeq 142$ MeV in the chiral limit from different prescriptions. A recent review contains a short introduction to the scaling window in QCD, and summarises these and other studies [47].

In this study we define an ad-hoc order parameter, which we dub $\langle \bar{\psi}\psi \rangle_3$, free from contributions linear in mass [48]. We explore a range of masses and temperatures, in an attempt to identify the limits of the scaling window, and its possible cross-over to a mean field behaviour. A very preliminary account of some of the results has been presented in Ref. [3].

2. Observables, magnetic Equation of State, and scaling

A quantitative way to describe a critical system with a breaking field h relies on the EoS for the order parameter M

$$M = h^{1/\delta} f(t/h^{1/\beta\delta}). \quad (1)$$

In the Eq. (1) we identify $M \equiv \langle \bar{\psi}\psi \rangle$, $h \equiv m_l$, $t \equiv (T - T_0)$, where m_l is the light quark mass and $T_0 \equiv T_c(m_l \rightarrow 0)$ is the critical temperature in the chiral limit, δ and β are critical exponents. Note that there are two independent normalizations for M and for t , which, like T_0 , depend on the strange quark mass. In our range of masses it is legitimate to trade $m_l \simeq m_\pi^2$, with a suitable adjustment of normalizations. $f(x)$, with $x = t/h^{1/\beta\delta}$, is a universal curve for a given breaking pattern.

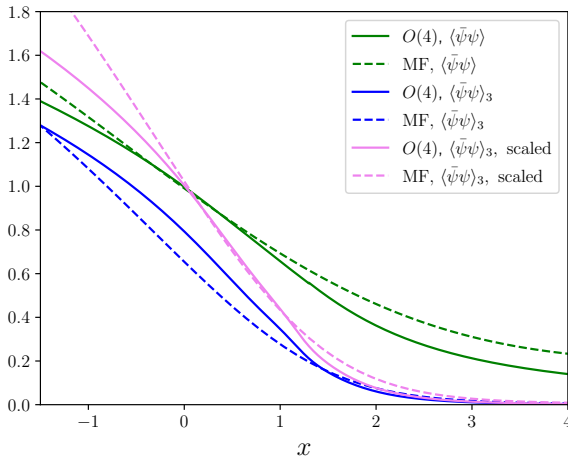


Figure 1: The Equation of State for the chiral condensate $\langle \bar{\psi}\psi \rangle$ and for the new order parameter $\langle \bar{\psi}\psi \rangle_3$ in the critical region for the 3D $O(4)$ universality class, and for the mean field. For a more direct comparison we also plot the results, normalised so that they coincide at $x = 0$, as purple lines.

For the 3D $O(4)$ scaling function we rely on the parameterization from Ref. [49] as well as on its polynomial interpolation [50, 51], which is smooth in the critical region. A successful scaling of results for a finite mass would identify the critical

temperature in the chiral limit, besides confirming universality. One less stringent approach to scaling relies on pseudo-critical temperatures associated with features of the order parameter. Consider the two susceptibilities: $\chi_L = \frac{\partial \langle \bar{\psi}\psi \rangle}{\partial m_l}$ and $\chi_\Delta = \frac{\partial \langle \bar{\psi}\psi \rangle}{\partial T}$, which peak at $t/h^{1/\beta\delta} = 1.35(3)$ and $t/h^{1/\beta\delta} = 0.74(4)$, respectively, for 3D $O(4)$ universality class with the critical exponents $\delta = 4.8(1)$ and $\beta = 0.38(1)$. The peak positions define pseudo-critical temperatures

$$T_c(m_\pi) = T_0 + A z_p m_\pi^{2/\beta\delta}. \quad (2)$$

A is a mass independent parameter, and T_c for different observables should scale with the same exponent $2/\beta\delta$, but with different z_p 's.

2.1. A new order parameter

In the same spirit as Ref. [52], we consider the transverse $\chi_T = \frac{\langle \bar{\psi}\psi \rangle}{m_l}$ and longitudinal $\chi_L = \frac{\partial \langle \bar{\psi}\psi \rangle}{\partial m_l}$ susceptibilities and their difference $O_{LT} \equiv \chi_T - \chi_L$. O_{LT} is an order parameter for the transition, since $\chi_L = \chi_T$ in the chiral limit in the symmetric phase. Moreover, by construction, any linear contribution in m_l – either coming from the regular part of the EoS or from additive renormalization – drops from the difference. However O_{LT} is divergent in the chiral limit in the broken phase. The singularity is avoided by defining:

$$\langle \bar{\psi}\psi \rangle_3 \equiv \langle \bar{\psi}\psi \rangle - m_l \chi_L \equiv \langle \bar{\psi}\psi \rangle - m_l \frac{\partial \langle \bar{\psi}\psi \rangle}{\partial m_l}. \quad (3)$$

This is the order parameter, whose Taylor expansion in m_l – when defined – starts at a third order, as noted in Ref. [48].

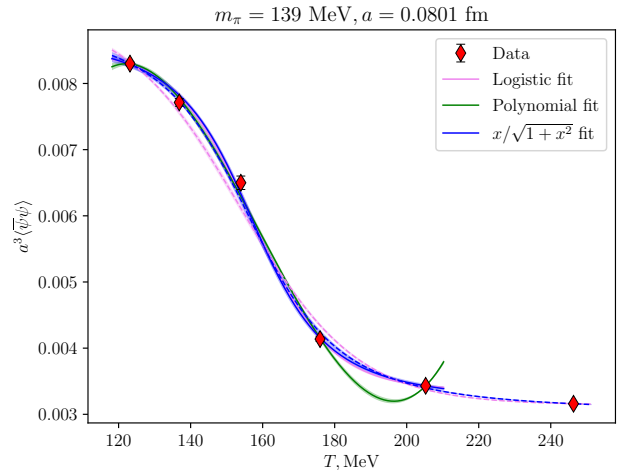


Figure 2: Chiral condensate (5) as a function of temperature T . Solid lines indicate the fit in the range [120 : 210] MeV, dashed lines correspond to the range [120 : 250] MeV.

Deriving the Equation of State for $\langle \bar{\psi}\psi \rangle_3$ is straightforward:

$$\frac{\langle \bar{\psi}\psi \rangle_3}{m_l^{1/\delta}} = f(x)(1 - 1/\delta) + \frac{x}{\beta\delta} f'(x). \quad (4)$$

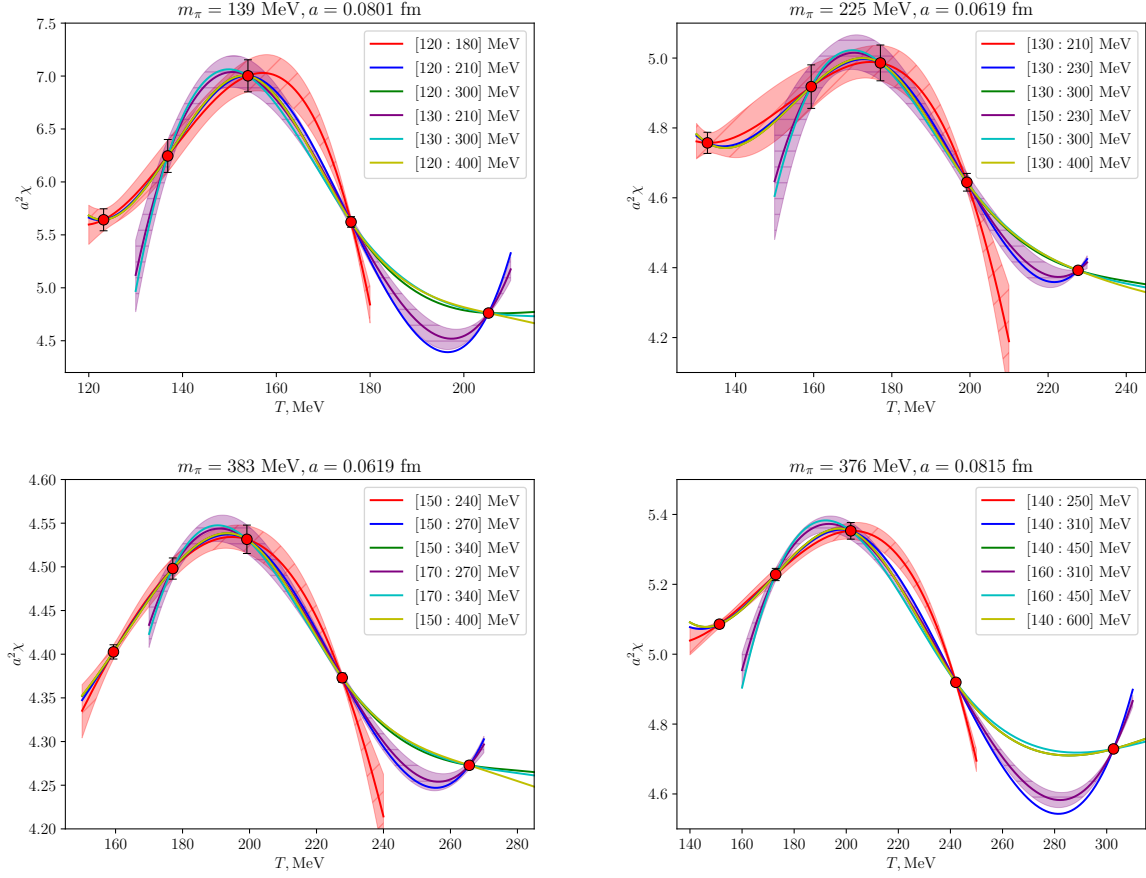


Figure 3: Chiral susceptibility as a function of temperature and its cubic spline interpolation. In some cases we also display the statistical errors, see the text.

The high temperature leading term is $\langle \bar{\psi}\psi \rangle_3 \propto t^{-\gamma-2\beta\delta}$ rather than $\langle \bar{\psi}\psi \rangle \propto t^{-\gamma}$: the decay is rather fast. The inflection point that drives the behaviour of the pseudo-critical temperature associated with $\langle \bar{\psi}\psi \rangle_3$ is $x_{\text{infl}} = 0.55(1)$. Note that the pseudo-critical temperature for this observable follows the same scaling in Eq. (2), but with a smaller z_p : this means that the pseudo-critical temperature associated with the inflection point of $\langle \bar{\psi}\psi \rangle_3$ is smaller than the pseudo-critical temperatures associated with chiral condensate and susceptibility. This also implies that it is closer to the true critical one in the limit $m_l \rightarrow 0$.

In Fig. 1 we compare the EoS for $\langle \bar{\psi}\psi \rangle_3$ with the one for $\langle \bar{\psi}\psi \rangle$ for the $O(4)$ Universality class and for the mean field. We note the sharper decrease of $\langle \bar{\psi}\psi \rangle_3$, very understandable given that it is closer to the chiral condensate in the chiral limit, followed by the high temperature behaviour just described. For either observable we also show the mean field result: it is indeed very close to the 3D $O(4)$, so the transition from the scaling window to a regime with small fluctuations is expected to be very smooth.

3. Numerical results

In this work we present new results for the physical pion mass, together with an extended analysis of the results for higher pion masses [5]. Simulations are performed in the fixed scale

TMFT	ETMC	m_π [MeV]	a [fm]	Z_p
M140	cB211.072.64	139.3(7)	0.0801(4)	0.462(4)
D210	D15.48	225(5)	0.0619(18)	0.516(2)
D370	D45.32	383(11)	0.0619(18)	0.516(2)
B370	B55.32	376(14)	0.0815(30)	0.509(4)

Table 1: Parameters of the $N_f = 2 + 1 + 1$ gauge fields ensembles used for the analysis. Lattice spacing and pion mass for D and B ensembles are taken from [53], renormalization factor Z_p for these ensembles was measured in [54]. All parameters of the M ensemble are from [55]. The strange and charm quark masses are close to their physical values.

approach, where we keep the bare lattice parameters fixed and vary the temperature by varying the number of lattice points in the temporal direction N_t . Gauge fields ensembles used in this paper are summarized in Table 1. New simulations for the physical pion mass use Wilson-clover twisted mass fermions, with the parameters of the action corresponding to the zero temperature ensemble cB211.072.064 of ETMC [56]. The number of configurations generated for these ensembles is given in Table 2. First results of our simulations with physical pion mass were presented in [3].

The chiral condensate is an (approximate) order parameter

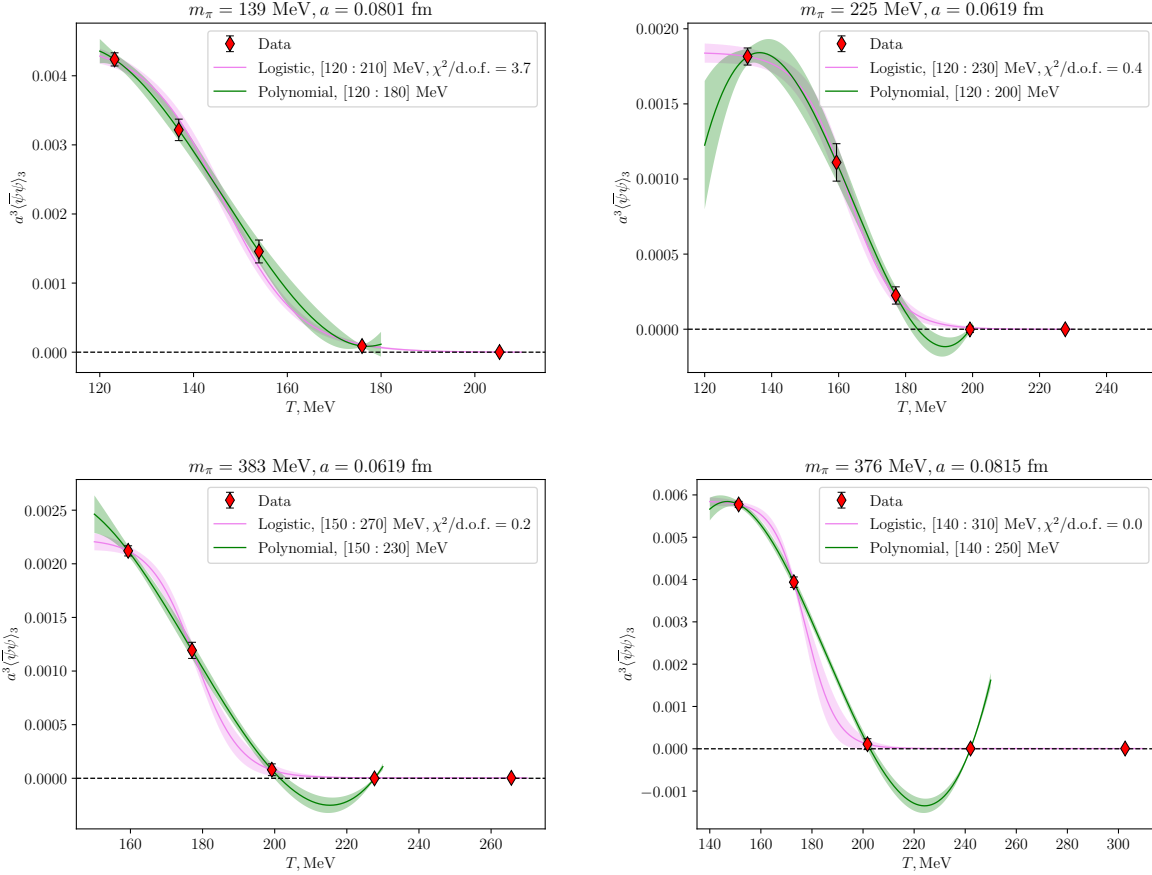


Figure 4: (Bare) $\langle\bar{\psi}\psi\rangle_3$ as a function of temperature T , for ensembles as indicated, and fits superimposed; see text for details.

N_t	T [MeV]	# conf	N_t	T [MeV]	# conf
20	123(1)	782	10	246(1)	592
18	137(1)	892	8	308(2)	498
16	154(1)	534	6	411(2)	195
14	176(1)	359	4	616(3)	472
12	205(1)	337			

Table 2: Statistics of the physical pion mass ensembles M140. Each fourth molecular dynamics trajectory was saved.

for the chiral symmetry in the light quark sector:

$$\langle\bar{\psi}\psi\rangle = \langle\bar{u}u\rangle + \langle\bar{d}d\rangle = \frac{T}{V} \frac{\partial Z}{\partial m_l} = \frac{1}{N_t N_s^3} \langle\text{tr } M^{-1}\rangle. \quad (5)$$

In numerical simulations the trace of M^{-1} was measured using noisy stochastic estimator with 24 random volume sources. It is important to note that the bare chiral condensate (5) should be renormalized. However, in the fixed scale approach, applied in this paper, both additive and multiplicative renormalization factors are equal for all points. Thus, the renormalization procedure has no effect on the pseudo-critical temperatures extracted from the peak of χ_Δ , or, equivalently, from the inflection point of the chiral condensate.

In Fig. 2 we present the dependence of the chiral conden-

sate (5) on the temperature for the physical pion mass. We extract the pseudo-critical temperature T_Δ from the inflection point of this dependence. For this purpose we fitted the chiral condensate with several functions, varying fitting interval:

- Logistic: $A + B \tanh \frac{T-T_\Delta}{\delta T_\Delta}$,
- $A + B \frac{T-T_\Delta}{\sqrt{\delta T^2 + (T-T_\Delta)^2}}$,
- Polynomial: $\Delta = a_\Delta + b_\Delta T + c_\Delta T^2 + d_\Delta T^3$.

We find that the quality of the fit worsens when the upper limit approaches 300 MeV. The final estimation is obtained by averaging over three functional forms and two fitting intervals [120:210] and [120:250] MeV (apart from the polynomial fit, which describes the data poorly at large interval [120:250] MeV). The difference between various functions/intervals was used to estimate the systematic uncertainty. The final results for the pseudo-critical temperature T_Δ are quoted in Table 3. The results for heavier pion masses are from our previous analysis [5].

The chiral susceptibility, which is defined as the mass derivative of the chiral condensate $\chi_L = \frac{\partial}{\partial m_l} \langle\bar{\psi}\psi\rangle$, consists of con-

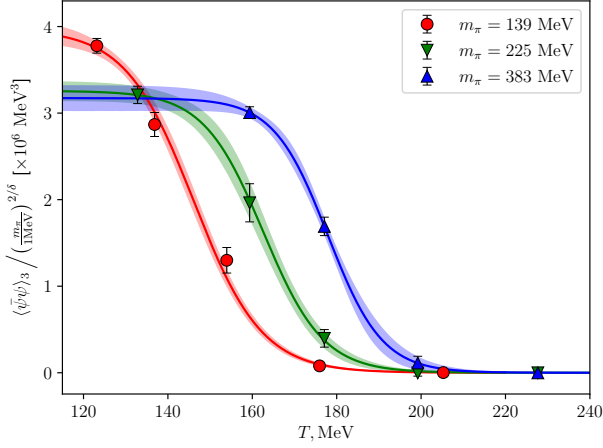


Figure 5: Search for the $O(4)$ scaling of $\langle \bar{\psi}\psi \rangle_3$: at the critical temperature, $\frac{\langle \bar{\psi}\psi \rangle_3}{m_\pi^{2/\delta}}$ does not depend on the quark mass. The crossing point of the results for the two lightest masses picks a candidate critical temperature $T_0^\delta = 138(2)$ MeV.

ected χ_{conn} and disconnected χ_{disc} contributions:

$$\begin{aligned} \chi_L &= \frac{\partial}{\partial m_l} \langle \bar{\psi}\psi \rangle = \chi_{\text{disc}} + \chi_{\text{conn}}, \\ \chi_{\text{disc}} &= \frac{T}{V} \left(\langle (\text{tr } M^{-1})^2 \rangle - \langle \text{tr } M^{-1} \rangle^2 \right), \\ \chi_{\text{conn}} &= -\frac{T}{V} \langle \text{tr } M^{-2} \rangle. \end{aligned} \quad (6)$$

Also, the chiral susceptibility suffers from additive and multiplicative renormalizations, which, again, are not affecting the estimate of the pseudo-critical point.

In Fig. 3 we show the chiral susceptibility for all ensembles. We note that this observable has a strong regular contribution, in addition to an additive renormalization. These features are qualitatively clear in the plots: rather than the simple symmetric shape predicted by the EoS, the curves are skewed and have a long high temperature tail. For this reason, and given a small number of points in the transition region, we decided to use a model independent estimate of the pseudo-critical temperature, based on cubic spline interpolation, instead of using an explicit functional form. To estimate the statistical uncertainty we added random Gaussian noise to each point, with the amplitude given by the statistical uncertainty of our data points. Typically we used $O(2000)$ splines for error estimate, and we find this a rather robust procedure. The dispersion of the different results can be appreciated from the plots, and we show the statistical errors in a few selected cases - the others behave similarly.

Finally we compute $\langle \bar{\psi}\psi \rangle_3$ as in (3). As discussed above in Section 2, $\langle \bar{\psi}\psi \rangle_3$ is free from linear additive renormalization as well as from linear correction to scaling. It still needs a multiplicative renormalization, which is obviously the same Z_p as for the chiral condensate, Table 1.

The temperature dependence of $\langle \bar{\psi}\psi \rangle_3$ is shown in Fig. 4. We used several functional forms to fit the temperature depen-

dence of this observable, which shows a fast fall-off with temperature. We then find that the logistic curve is able to capture the behaviour for a sizeable range, while polynomial fits are limited to a few points. Upon the fit we tried to keep the fit interval fixed in units T/T_c : for logistic fit the interval is roughly $[0.8, 1.5]$, for polynomial $[0.8, 1.25]$. We used both functional forms to estimate the pseudo-critical temperature and its systematic uncertainty. The final results for the pseudo-critical temperature extracted from the chiral susceptibility and for $\langle \bar{\psi}\psi \rangle_3$ for all ensembles are presented in Table 3.

4. The magnetic Equation of State and $\langle \bar{\psi}\psi \rangle_3$

In Fig. 5 we show the results for $\langle \bar{\psi}\psi \rangle_3$ as a function of temperature, with superimposed logistic fits. The results are converted to physical units using the lattice spacing and the multiplicative renormalization given in Table 1 and divided by $m_\pi^{2/\delta}$, with δ fixed at the $O(4)$ value. At the critical temperature $\langle \bar{\psi}\psi \rangle_3 \propto m_\pi^{2/\delta}$, hence $\frac{\langle \bar{\psi}\psi \rangle_3}{m_\pi^{2/\delta}}$ should not depend on the mass at the critical point. The logic is similar to the one adopted in Refs. [33, 52] when searching for the fixed point of χ_L/χ_T . The crossing point of the curves for the lightest masses identifies a candidate critical temperature in the chiral limit, $T_0^\delta = 138(2)$ MeV, where the superscript δ refers to T_0 being estimated from the crossing point. Possible scaling violations would result in a mass dependence of T_0^δ .

Next, we fit to the 3D $O(4)$ EoS with open critical temperature. We rely on a smoothing spline to define the EoS and we introduce appropriate (pion mass dependent) scaling parameters: $g_{\text{fit}}(x) = ag \left(\frac{x - T_0^{\text{EoS}}}{b} \right)$, where $g(x)$ is given by EoS for the subtracted condensate in Eq. (4). In Fig. 6, left, we show the results in physical units, with $g_{\text{fit}}(x)$ superimposed as interpolating lines, which at a first sight look satisfactory. However the would-be critical temperatures T_0^{EoS} are not constant with mass, signaling residual scaling violations: we find $T_0^{\text{EoS}} = 142(2), 159(3), 174(2)$ MeV, from light to heavy masses. Only T_0^{EoS} for the physical pion mass is compatible with the previous estimate $T_0^\delta = 138(2)$ MeV, but there are obvious violations for larger masses. In the right-hand side of Fig. 6 we compare the mean field fits with the $O(4)$ EoS: as it was already clear from Fig. 1, they are very close to each other. In the smaller interval they basically coincide, only for the larger interval shown here, and for the lightest mass, $O(4)$ fits may be slightly favored.

Finally, in Fig. 7 we show high temperature fit of the condensate $\langle \bar{\psi}\psi \rangle_3$, constrained to the $O(4)$ behaviour: $\langle \bar{\psi}\psi \rangle_3 \propto t^{-\gamma-2\beta\delta}$ for $T_0 = 138$ MeV¹. The results are rescaled by $m_l^3 \simeq m_\pi^6$, the anticipated high temperature leading behaviour. In the interval of temperatures $160 \text{ MeV} < T < 300 \text{ MeV}$ (marked bold) the $O(4)$ prediction fares nicely through the data. For $T \gtrsim 300 \text{ MeV}$ the behaviour is distinctly different, and the data collapse on a single curve, as expected of the leading mass

¹The sensitivity to T_0 is very moderate here. T_0 itself is rather poorly constrained by the fit. For example, if one keeps T_0 as a free parameter, then the fit for the physical pion mass $m_\pi = 139$ MeV gives $T_0 = 132 \pm 4$ MeV in the interval $[150 : 300]$ MeV and $T_0 = 145.7 \pm 0.6$ MeV in the interval $[160 : 340]$ MeV.

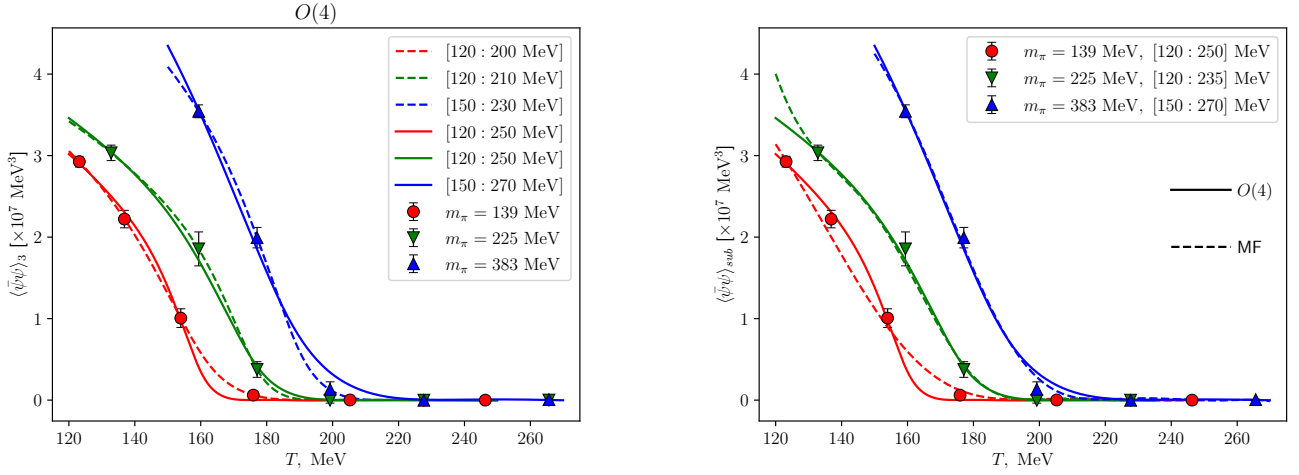


Figure 6: Fits to the Equation of State: 3D $O(4)$ (left), 3D $O(4)$ and mean field (right). For $m_\pi = 139$ MeV the critical temperature $T_0^{\text{EoS}} = 142(2)$ MeV is consistent with that estimated from the chiral extrapolation of the pseudo-critical temperatures (left); the data are compatible with mean field, with a mild tension building up for the physical pion mass (right).

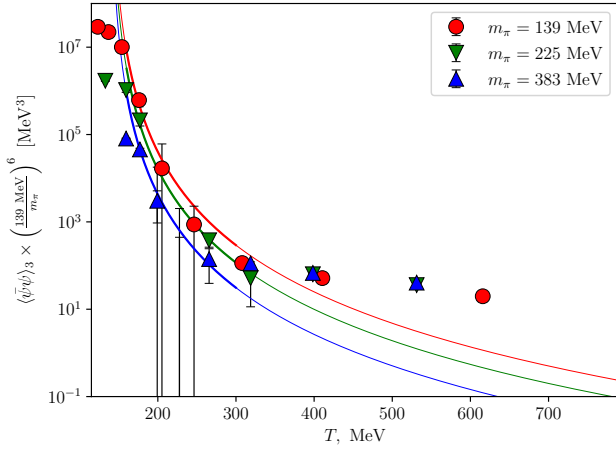


Figure 7: Fits to a constrained 3D $O(4)$ behaviour for the different pion masses: the results in the interval of temperatures [160:300] MeV (marked bold) fare nicely through the data. For $T > 300$ MeV the behaviour is distinctly different, and the data follows $m_l^3 \approx m_\pi^6$, the anticipated high temperature leading behaviour. $\chi^2/\text{d.o.f.}$ of the fit is 0.5/0.7/0.7 for pion masses $m_\pi = 139, 225$ and 383 MeV correspondingly.

term according to Griffith analyticity, regardless the critical behaviour. This suggests that the temperature extent of the scaling window above T_0 extends up to about 300 MeV. Interestingly, in a previous study [5] we have found that this is also the threshold for a dilute instanton gas behaviour.

5. The scaling of the pseudo-critical temperatures and the chiral limit

In the summary Table 3 we present all pseudocritical temperatures. The results on the B ensembles help monitoring the finite spacing effects, and we confirm that they are small also

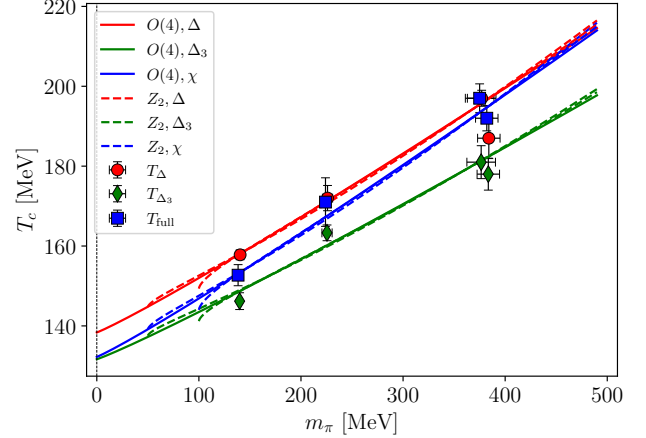


Figure 8: Pseudocritical temperatures from the chiral observables with superimposed the 3D $O(4)$ and Z_2 scaling fits described in the text. $\chi^2/\text{d.o.f.}$ for $O(4)$ fit is $\chi^2/\text{d.o.f.} = 2.1/1.0/2.5$ for the chiral condensate Δ , for the chiral susceptibility χ and the new observable Δ_3 . For Z_2 fits the $\chi^2/\text{d.o.f.}$ differs by maximum 20% from $\chi^2/\text{d.o.f.}$ of $O(4)$ fit.

for the new observables introduced here. A more detailed discussions on the continuum limit can be found in Ref. [5] as well as in ETMC papers, see e.g. Ref. [57], and references therein.

As discussed, we fit the pseudo-critical temperatures to a power law in the pion mass, see Eq. (2), where z_p is tabulated for the different observables in Table 4, A is a universal constant depending on the normalization scales, and $T_0 \equiv T_c(m_\pi \rightarrow 0)$ corresponds to the critical temperature in the chiral limit. We kept $2/(\beta\delta) = 1.083$ fixed to the value given by $O(4)$ critical exponents. In Table 4 we present T_0 and ratio of z_p extracted from the fit as well as the prediction of $O(4)$ scaling. There is a semi-quantitative agreement with $O(4)$ when considering the relative slopes of $\langle \bar{\psi}\psi \rangle$ and $\langle \bar{\psi}\psi \rangle_3$. When considering only the

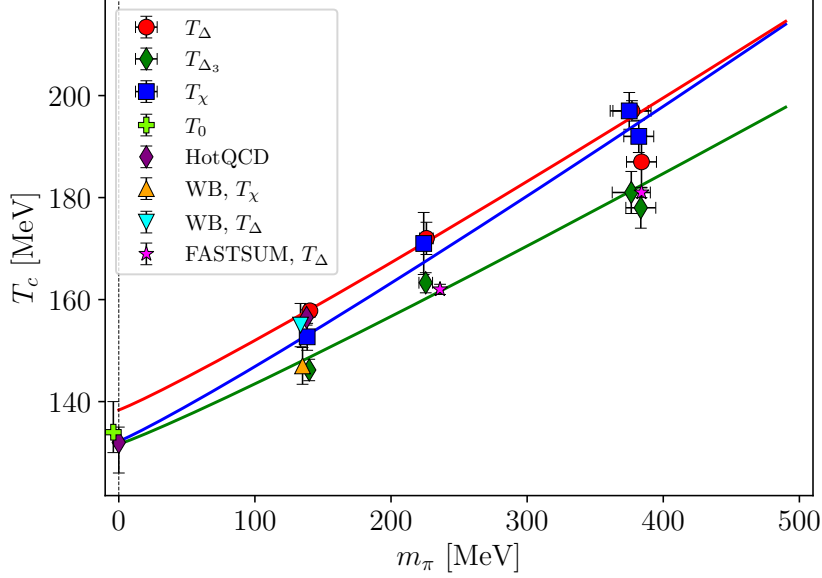


Figure 9: Pseudo-critical temperatures with their chiral extrapolations: comparison with the results from the HotQCD Collaboration [58], FASTSUM Collaboration [28, 29], Wuppertal-Budapest Collaboration [59]. The purple diamond at $m_\pi = 0$ marks the critical temperature [30] which compares well with our result $T_0 = 134^{+6}_{-4}$ MeV (light-green cross, slightly shifted for better readability).

Ensemble	T_Δ	T_{Δ_3}	T_χ
M140	157.8(7)(10)	146.2(21)(1)	152.7(13)(23)
D210	172(3)(1)	163.3(18)(8)	171(6)(1)
D370	187(5)(1)	178(4)(0)	192(3)(1)
B370	197(2)(0)	181(1)(4)	197(2)(3)

Table 3: Pseudo-critical temperature extracted from the chiral observables.

results for physical pion mass, with a critical temperature in the chiral limit within an acceptable range, $z_p/z_p(\bar{\psi}\psi_3) = 1.46$, with a large error.

Observable	T_0 [MeV]	$z_p/z_{\bar{\psi}\psi_3}$	$z_p/z_{\bar{\psi}\psi_3} O(4)$	$z_p O(4)$
χ	132(4)	1.24(17)	2.45(4)	1.35(3)
$\langle\bar{\psi}\psi\rangle$	138(2)	1.15(24)	1.35(7)	0.74(4)
$\langle\bar{\psi}\psi\rangle_3$	132(3)	1	1	0.55(1)

Table 4: Critical temperature in the chiral limit T_0 and the ratio of z_p extracted from the fit by Eq. (2). Last two columns contain predictions for z_p from 3D $O(4)$ scaling. Errors are only statistical.

The average of the extrapolated values of T_c in the chiral limit

$$T_0 \equiv T_c(m_\pi \rightarrow 0) = 134^{+6}_{-4} \text{ MeV} \quad (7)$$

is compatible with the estimated from the crossing point $T_0^\delta = 138(2)$ MeV, and only slightly below the estimate from the EoS for physical pion mass. This last point is consistent with the physical pion mass being close to the scaling window. Note that the error in Eq. (7) contains also systematic uncertainty, coming from extrapolation of different observables.

Similarly to Ref. [7] we also consider the breaking pattern corresponding to an effective restoration of the axial symmetry

$U(2)_L \times U(2)_R \rightarrow U(2)_V$, leading either to a second order transition with $\delta = 4.3(1), \beta = 0.40(4)$ or of first order transition, in which case the pseudo-critical behaviour would be driven by an endpoint in the Z_2 universality class. In the first case the exponents are close to the $O(4)$ ones and within our errors the results are indistinguishable. For the first order scenario we rely on the experience gathered with three-flavor QCD, where it was found that the mixing associated with the critical endpoint could well be low [60]. Hence, as in Ref. [7], we ignore the mixing and fit to

$$T_c(m_\pi) = T_0 + B(m_\pi^2 - m_c^2)^{1/\beta\delta} \quad (8)$$

with $1/\beta\delta = 0.64$ for the Z_2 3D universality class [61]. Also in this case, the critical exponents for $O(4)$ and Z_2 behaviour are close to each other, and it is very difficult to distinguish between these two scenarios. One can clearly see from Fig. 8 that the data can be also described with Z_2 behaviour and critical mass up to $m_c \sim 100$ MeV. If, artificially, we constrained $m_c = 0$, the lines would be indistinguishable from $O(4)$. All in all, we concur with other observations [1, 33] that extrapolation alone does not suffice to discriminate among different scenarios. A possible way to distinguish between different universal behaviours would include simulations with lower pion masses [30]. On the positive side, the extrapolated values of the pseudo-critical temperatures T are robust (up to the critical pion mass m_{cr}^π) against the choice of critical exponents.

In Fig. 9 we compare our estimations of the pseudo-critical temperature with the results obtained by staggered [58, 59] and Wilson [28, 29] fermions. The nice agreement of our results with others can be appreciated. We also superimpose $O(4)$ fits to our pseudo-critical temperatures and present our estimation of T_0 in the chiral limit which compares well with the estimations of HotQCD Collaboration [30].

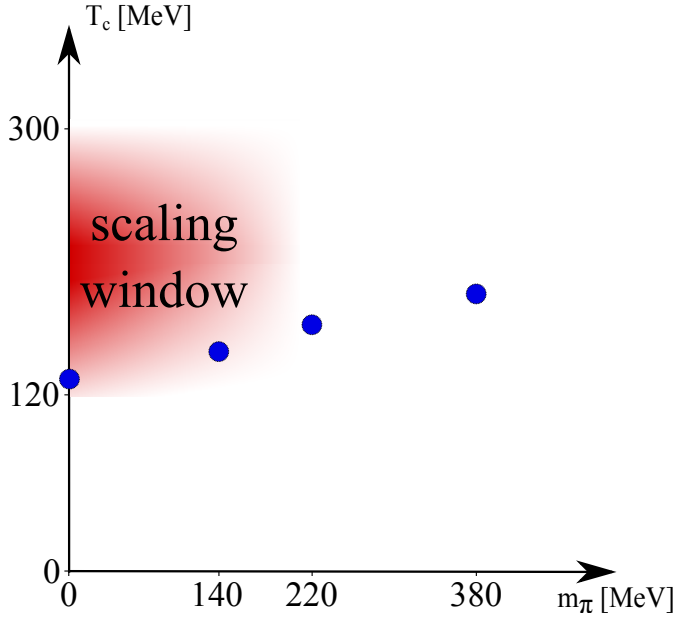


Figure 10: Sketch of the critical region: the critical temperature in the chiral limit T_0 is constrained from above from the pseudocritical temperature $T_{\Delta_3} = 146(2)$ MeV. The averaged extrapolation $T_0 = 134^{+6}_{-4}$ MeV satisfies this bound, and it is robust against different choices of critical scaling. It compares well with the estimate from anomalous scaling $T_0^\delta = 138(2)$ MeV. The different red shades indicate the compatibility with $O(4)$ scaling. The labels indicate the pion masses that we have investigated, for temperatures ranging from 120 MeV till 500 MeV.

6. Summary

The chiral behaviour of the QCD transition is a difficult, much studied problem. Direct tests of universality are hampered by scaling violations, and by the similarity among different scenarios. Here we have tackled these issues by introducing an order parameter, whose behaviour is closer to the critical one, hence with a reduced contribution from scaling violating terms; and by exploring a larger parameter region, with the goal to follow the evolution from a scaling behaviour till a regular one, unrelated with criticality.

Particularly interesting is the behaviour with physical quark masses. We have measured the pseudo-critical temperature for three different observables, finding critical temperatures in agreement with staggered estimates for the chiral condensate and the chiral susceptibility. The new order parameter $\langle \bar{\psi}\psi \rangle_3$ gives a lower pseudo-critical temperature $T_{\Delta_3} = 146.2(21)(1)$ MeV, in accordance with its being closer to the true critical behaviour. We have used three different strategies for the computation of the critical temperature in the chiral limit: the first one is based on the scaling of $\langle \bar{\psi}\psi \rangle_3$ at the critical temperature $T_0(m_\pi = 0)$, the second one is based on the fit of $\langle \bar{\psi}\psi \rangle_3$ to the magnetic Equation of State, which should give the value of T_0 for each single pion mass, barring scaling violations, the last one is based on extrapolation of the pseudo-critical temperatures extracted from different observables to the chiral limit. A search for the anomalous scaling of $\langle \bar{\psi}\psi \rangle_3$ at the chiral transition picks the critical

temperature of $T_0 = 138(2)$ MeV. For all the masses the results are apparently well described by the universal EoS, however only for the physical pion mass the estimated critical temperature $T_0 = 142(2)$ MeV approaches the results obtained by extrapolation, $T_0 = 134^{+6}_{-4}$ MeV. We note that the pseudo-critical temperature $T_{\Delta_3} = 146.2(21)(1)$ MeV for a physical pion mass serves as an upper bound for the critical temperature. As a final result for the critical temperature we quote $T_0 = 134^{+6}_{-4}$ MeV. In Fig. 9 we present our results for the pseudo-critical temperatures, their chiral extrapolation and comparison to the results of other groups, with which we find a nice agreement.

For larger masses the 3D $O(4)$ EoS fits are indistinguishable from mean field, while a mild tension appears for the physical mass, with $O(4)$ slightly favoured. The high temperature behaviour shows a clear threshold at temperatures about 300 MeV, above which a trend consistent with $O(4)$ scaling gives way to a simple leading order analytic scaling dictated by Griffith analyticity. As a side comment, in a previous study [5] we have found that this is also the threshold for a dilute instanton gas behaviour. A threshold around the same temperature was also observed in other lattice studies[62–64]. Our observations are compatible with an onset of scaling around the physical value of the pion mass, and temperatures below 300 MeV. In Fig. 10 we sketch the critical region, highlighting the compatibility with $O(4)$ scaling. Our results seem to be in contradiction with the results of [21, 46], where scaling is observed only for very tiny pion masses. Possible sources of this discrepancy and connection to the presented results are the subject of future work and will be discussed elsewhere.

We also studied the possibility of first order phase transition in the chiral limit, in which case the observables are expected to scale according to Z_2 universality class with some critical pion mass m_c . Our data can be also described with Z_2 behaviour and critical mass up to $m_c \sim 100$ MeV. Thus we conclude that extrapolation alone does not suffice to discriminate among different scenarios. Similar conclusions were reached in the two flavor model [7]. A possible way to distinguish between different universal behaviour would include simulations with lower pion masses [30, 33], hoping to observe directly a first order transition. While a direct observation of such a first order transition would settle the issue, a lack of observation makes it difficult to exclude that such a transition appears at very low masses. We hope that by exploiting more the universal properties of the Equation of State, possibly using some of the strategies outlined here, and in comparison with analytic approaches, may provide a more solid answer.

It would also be interesting to repeat a similar analysis using staggered results for pion masses smaller than physical [33] as well as with FRG results [21]. Also, Fig. 1 suggests that results below the critical temperature in the chiral limit may be useful to further discriminate true critical behaviour from mean field.

This work should be ameliorated and extended along several lines: we have not performed a continuum limit extrapolation. The indirect checks performed by the ETMC collaboration as well as by ourselves [5], and the good consistency of the results at the larger mass, see Table 3, give some confidence that residual spacing corrections should not exceed a few per-

cent. The fixed scale approach has several advantages, but we have to rely heavily on interpolations. Results on finer lattices should also help in this respect, by producing results at intermediate temperatures. Since the ETM Collaboration has recently released a new set of zero temperature tuned parameters [57], we hope to return to this point in the future. Finally, we have completed an analysis of correlators and screening masses on the configurations for physical pion mass, to complement the discussion on chiral and axial symmetry, and the results will appear soon [65].

Acknowledgements

We thank Frithjof Karsch, Anirban Lahiri, Jan Pawłowski and Wolfgang Unger for valuable discussions and correspondence. This work uses the ETMC public code, and we are grateful to the ETM Collaboration, in particular to Roberto Frezzotti, Karl Jansen and Carsten Urbach, for helpful discussions on several aspects of the twisted mass formulation. This work is partially supported by STRONG-2020, a European Union’s Horizon 2020 research and innovation programme under grant agreement No. 824093. The work of A.Yu.K. and A.T. was supported by RFBR grant 18-02-40126. A.T. acknowledges support from the “BASIS” foundation. Numerical simulations have been carried out using computing resources of CINECA (based on the agreement between INFN and CINECA, on the ISCRa project IsB20), the supercomputer of Joint Institute for Nuclear Research “Govorun”, and the computing resources of the federal collective usage center Complex for Simulation and Data Processing for Mega-science Facilities at NRC “Kurchatov Institute”, <http://ckp.nrcki.ru/>.

References

- [1] Heng-Tong Ding. New developments in lattice QCD on equilibrium physics and phase diagram. In *28th International Conference on Ultra-relativistic Nucleus-Nucleus Collisions*, 2 2020, 2002.11957.
- [2] Jana N. Guenther. Overview of the QCD phase diagram: Recent progress from the lattice. *Eur. Phys. J. A*, 57(4):136, 2021.
- [3] Andrey Yu. Kotov, Maria Paola Lombardo, and Anton M. Trunin. Finite temperature QCD with $N_f = 2 + 1 + 1$ Wilson twisted mass fermions at physical pion, strange and charm masses. *Eur. Phys. J.*, A56(8):203, 2020, 2004.07122.
- [4] Andrey Yu. Kotov, Maria Paola Lombardo, and Anton M. Trunin. Fate of the η' in the quark gluon plasma. *Phys. Lett. B*, 794:83–88, 2019, 1903.05633.
- [5] Florian Burger, Ernst-Michael Ilgenfritz, Maria Paola Lombardo, and Anton Trunin. Chiral observables and topology in hot QCD with two families of quarks. *Phys. Rev. D*, 98(9):094501, 2018, 1805.06001.
- [6] Florian Burger, Ernst-Michael Ilgenfritz, Maria Paola Lombardo, Michael Müller-Preussker, and Anton Trunin. Topology (and axion’s properties) from lattice QCD with a dynamical charm. *Nucl. Phys. A*, 967:880–883, 2017, 1705.01847.
- [7] Florian Burger, Ernst-Michael Ilgenfritz, Malik Kirchner, Maria Paola Lombardo, Michael Müller-Preussker, Owe Philipsen, Carsten Urbach, and Lars Zeidlewicz. Thermal QCD transition with two flavors of twisted mass fermions. *Phys. Rev. D*, 87(7):074508, 2013, 1102.4530.
- [8] Robert D. Pisarski and Frank Wilczek. Remarks on the Chiral Phase Transition in Chromodynamics. *Phys. Rev. D*, 29:338–341, 1984.
- [9] Krishna Rajagopal and Frank Wilczek. Static and dynamic critical phenomena at a second order QCD phase transition. *Nucl. Phys. B*, 399:395–425, 1993, hep-ph/9210253.
- [10] Andrea Pelissetto and Ettore Vicari. Relevance of the axial anomaly at the finite-temperature chiral transition in QCD. *Phys. Rev. D*, 88(10):105018, 2013, 1309.5446.
- [11] Ken Kawarabayashi and Nobuyoshi Ohta. The Problem of η in the Large N Limit: Effective Lagrangian Approach. *Nucl. Phys.*, B175:477–492, 1980.
- [12] Ken Kawarabayashi and Nobuyoshi Ohta. On the Partial Conservation of the U(1) Current. *Prog. Theor. Phys.*, 66:1789, 1981.
- [13] Angel Gómez Nicola, Jacobo Ruiz De Elvira, and Andrea Vioque-Rodríguez. The QCD topological charge and its thermal dependence: the role of the η' . *JHEP*, 11:086, 2019, 1907.11734.
- [14] Davor Horvatić, Dalibor Kekez, and Dubravko Klabužar. η' and η mesons at high T when the $U_A(1)$ and chiral symmetry breaking are tied. *Phys. Rev. D*, 99(1):014007, 2019, 1809.00379.
- [15] Joseph I. Kapusta, Eral Rrapaj, and Serge Rudaz. Is Hyperon Polarization in Relativistic Heavy Ion Collisions Connected to Axial U(1) Symmetry Breaking at High Temperature? *Phys. Rev. C*, 101(3):031901, 2020, 1910.12759.
- [16] Joseph I. Kapusta, D. Kharzeev, and Larry D. McLerran. The Return of the prodigal Goldstone boson. *Phys. Rev. D*, 53:5028–5033, 1996, hep-ph/9507343.
- [17] Edward V. Shuryak. Which chiral symmetry is restored in hot QCD? *Comments Nucl. Part. Phys.*, 21(4):235–248, 1994, hep-ph/9310253.
- [18] Simon Resch, Fabian Rennecke, and Bernd-Jochen Schaefer. Mass sensitivity of the three-flavor chiral phase transition. *Phys. Rev. D*, 99(7):076005, 2019, 1712.07961.
- [19] Bernd-Jochen Schaefer and Mario Mitter. Three-flavor chiral phase transition and axial symmetry breaking with the functional renormalization group. *Acta Phys. Polon. Supp.*, 7(1):81–90, 2014, 1312.3850.
- [20] Fei Gao and Jan M. Pawłowski. QCD phase structure from functional methods. *Phys. Rev. D*, 102(3):034027, 2020, 2002.07500.
- [21] Jens Braun, Wei-jie Fu, Jan M. Pawłowski, Fabian Rennecke, Daniel Rosenblüh, and Shi Yin. Chiral susceptibility in $(2+1)$ -flavor QCD. *Phys. Rev. D*, 102(5):056010, 2020, 2003.13112.
- [22] Lukas Mazur, Olaf Kaczmarek, Edwin Laermann, and Sayantan Sharma. The fate of axial U(1) in $2+1$ flavor QCD towards the chiral limit. *PoS, LATTICE2018*:153, 2019, 1811.08222.
- [23] Sayantan Sharma. The fate of $U_A(1)$ and topological features of QCD at finite temperature. In *11th International Workshop on Critical Point and Onset of Deconfinement*, 1 2018, 1801.08500.
- [24] Hidenori Fukaya. Can axial U(1) anomaly disappear at high temperature? *EPJ Web Conf.*, 175:01012, 2018, 1712.05536.
- [25] Sayantan Sharma. The fate of $U_A(1)$ and topological features of QCD at finite temperature. *PoS, CPOD2017*:086, 2018.
- [26] Christian Schmidt and Sayantan Sharma. The phase structure of QCD. *J. Phys. G*, 44(10):104002, 2017, 1701.04707.
- [27] A. Tomiya, G. Cossu, S. Aoki, H. Fukaya, S. Hashimoto, T. Kaneko, and J. Noaki. Evidence of effective axial U(1) symmetry restoration at high temperature QCD. *Phys. Rev. D*, 96(3):034509, 2017, 1612.01908. [Addendum: Phys.Rev.D 96, 079902 (2017)].
- [28] Gert Aarts et al. Spectral quantities in thermal QCD: a progress report from the FASTSUM collaboration. In *37th International Symposium on Lattice Field Theory*, 2019, 1912.09827.
- [29] G. Aarts et al. Properties of the QCD thermal transition with $N_f = 2 + 1$ flavours of Wilson quark. *arXiv:2007.04188*, 2020.
- [30] H.T. Ding et al. Chiral Phase Transition Temperature in $(2+1)$ -Flavor QCD. *Phys. Rev. Lett.*, 123(6):062002, 2019, 1903.04801.
- [31] T. Umeda, S. Ejiri, R. Iwami, K. Kanaya, H. Ohno, A. Uji, N. Wakabayashi, and S. Yoshida. $O(4)$ scaling analysis in two-flavor QCD at finite temperature and density with improved Wilson quarks. *PoS, LATTICE2016*:376, 2017, 1612.09449.
- [32] S. Ejiri, F. Karsch, E. Laermann, C. Miao, S. Mukherjee, P. Petreczky, C. Schmidt, W. Soeldner, and W. Unger. On the magnetic equation of state in $(2+1)$ -flavor QCD. *Phys. Rev. D*, 80:094505, 2009, 0909.5122.
- [33] H. T. Ding, S. T. Li, Swagato Mukherjee, A. Tomiya, X. D. Wang, and Y. Zhang. Correlated Dirac Eigenvalues and Axial Anomaly in Chiral Symmetric QCD. *Phys. Rev. Lett.*, 126(8):082001, 2021, 2010.14836.
- [34] Olaf Kaczmarek, Lukas Mazur, and Sayantan Sharma. Eigenvalue spectra of QCD and the fate of $U_A(1)$ breaking towards the chiral limit. 2 2021, 2102.06136.
- [35] Olaf Kaczmarek, Frithjof Karsch, Anirban Lahiri, Lukas Mazur, and

- Christian Schmidt. QCD phase transition in the chiral limit. 3 2020, 2003.07920.
- [36] S. Aoki, Y. Aoki, H. Fukaya, S. Hashimoto, C. Rohrhofer, and K. Suzuki. Role of axial $U(1)$ anomaly in chiral susceptibility of QCD at high temperature. 3 2021, 2103.05954.
- [37] S. Aoki, Y. Aoki, G. Cossu, H. Fukaya, S. Hashimoto, T. Kaneko, C. Rohrhofer, and K. Suzuki. Study of the axial $U(1)$ anomaly at high temperature with lattice chiral fermions. *Phys. Rev. D*, 103(7):074506, 2021, 2011.01499.
- [38] Michael I. Buchoff, Michael Cheng, Norman H. Christ, H.-T. Ding, Chulwoo Jung, F. Karsch, Zhongjie Lin, R. D. Mawhinney, Swagato Mukherjee, P. Petreczky, Dwight Renfrew, Chris Schroeder, P. M. Vranas, and Hantao Yin. Qcd chiral transition, $u(1)_A$ symmetry and the dirac spectrum using domain wall fermions. *Phys. Rev. D*, 89:054514, Mar 2014, 1309.4149.
- [39] Kei Suzuki, Sinya Aoki, Yasumichi Aoki, Guido Cossu, Hidenori Fukaya, Shoji Hashimoto, and Christian Rohrhofer. Axial $U(1)$ symmetry and mesonic correlators at high temperature in $N_f = 2$ lattice QCD. In *37th International Symposium on Lattice Field Theory*, 1 2020, 2001.07962.
- [40] Takuya Kanazawa and Naoki Yamamoto. $U(1)$ axial symmetry and Dirac spectra in QCD at high temperature. *JHEP*, 01:141, 2016, 1508.02416.
- [41] Sinya Aoki, Hidenori Fukaya, and Yusuke Taniguchi. Chiral symmetry restoration, eigenvalue density of Dirac operator and axial $U(1)$ anomaly at finite temperature. *Phys. Rev. D*, 86:114512, 2012, 1209.2061.
- [42] Bastian B. Brandt, Marco Cè, Anthony Francis, Tim Harris, Harvey B. Meyer, Hartmut Wittig, and Owe Philipsen. Testing the strength of the $U_A(1)$ anomaly at the chiral phase transition in two-flavour QCD. *PoS, CD2018:055*, 2019, 1904.02384.
- [43] Bastian B. Brandt, Anthony Francis, Harvey B. Meyer, Owe Philipsen, Daniel Robaina, and Hartmut Wittig. On the strength of the $U_A(1)$ anomaly at the chiral phase transition in $N_f = 2$ QCD. *JHEP*, 12:158, 2016, 1608.06882.
- [44] Guido Cossu, Sinya Aoki, Hidenori Fukaya, Shoji Hashimoto, Takashi Kaneko, Hideo Matsufuru, and Jun-Ichi Noaki. Finite temperature study of the axial $U(1)$ symmetry on the lattice with overlap fermion formulation. *Phys. Rev. D*, 87(11):114514, 2013, 1304.6145. [Erratum: *Phys.Rev.D* 88, 019901 (2013)].
- [45] Ting-Wai Chiu, Wen-Ping Chen, Yu-Chih Chen, Han-Yi Chou, and Tung-Han Hsieh. Chiral symmetry and axial $U(1)$ symmetry in finite temperature QCD with domain-wall fermion. *PoS, LATTICE2013:165*, 2014, 1311.6220.
- [46] Jens Braun, Bertram Klein, and Piotr Piasecki. On the scaling behavior of the chiral phase transition in QCD in finite and infinite volume. *Eur. Phys. J. C*, 71:1576, 2011, 1008.2155.
- [47] Andrey Yu Kotov, Maria Paola Lombardo, and Anton Trunin. Gliding Down the QCD Transition Line, from $N_f = 2$ till the Onset of Conformality. *Symmetry*, 13(10):1833, 2021.
- [48] Wolfgang Unger. *The chiral phase transition of QCD with 2+1 flavors : a lattice study on Goldstone modes and universal scaling*. PhD thesis, U. Bielefeld (main), 2010.
- [49] Jurgen Engels and Tereza Mendes. Goldstone mode effects and scaling function for the three-dimensional $O(4)$ model. *Nucl. Phys.*, B572:289–304, 2000, hep-lat/9911028.
- [50] J. Engels and F. Karsch. The scaling functions of the free energy density and its derivatives for the 3d $O(4)$ model. *Phys. Rev.*, D85:094506, 2012, 1105.0584.
- [51] J. Engels, L. Fromme, and M. Seniuch. Correlation lengths and scaling functions in the three-dimensional $O(4)$ model. *Nucl. Phys.*, B675:533–554, 2003, hep-lat/0307032.
- [52] Aleksandar Kocic, John B. Kogut, and Maria-Paola Lombardo. Universal properties of chiral symmetry breaking. *Nucl. Phys.*, B398:376–404, 1993, hep-lat/9209010.
- [53] Markus Werner et al. Hadron-Hadron Interactions from $N_f = 2+1+1$ Lattice QCD: The ρ -resonance. *Eur. Phys. J.*, A56(2):61, 2020, 1907.01237.
- [54] N. Carrasco et al. Up, down, strange and charm quark masses with $N_f = 2+1+1$ twisted mass lattice QCD. *Nucl. Phys.*, B887:19–68, 2014, 1403.4504.
- [55] C. Alexandrou et al. Nucleon axial and pseudoscalar form factors from lattice QCD at the physical point. *Phys. Rev. D*, 103(3):034509, 2021, 2011.13342.
- [56] Constantia Alexandrou et al. Simulating twisted mass fermions at physical light, strange and charm quark masses. *Phys. Rev.*, D98(5):054518, 2018, 1807.00495.
- [57] C. Alexandrou et al. Quark masses using twisted mass fermion gauge ensembles. 4 2021, 2104.13408.
- [58] A. Bazavov et al. Chiral crossover in QCD at zero and non-zero chemical potentials. *Phys. Lett.*, B795:15–21, 2019, 1812.08235.
- [59] Szabolcs Borsanyi, Zoltan Fodor, Jana N. Guenther, Ruben Kara, Sandor D. Katz, Paolo Parotto, Attila Pasztor, Claudia Ratti, and Kálman K. Szabó. Qcd crossover at finite chemical potential from lattice simulations. *Physical Review Letters*, 125(5), Jul 2020.
- [60] F. Karsch, C. R. Allton, S. Ejiri, S. J. Hands, O. Kaczmarek, E. Laermann, and C. Schmidt. Where is the chiral critical point in three flavor QCD? *Nucl. Phys. B Proc. Suppl.*, 129:614–616, 2004, hep-lat/0309116.
- [61] Ettore Vicari and Haralambos Panagopoulos. Theta dependence of $SU(N)$ gauge theories in the presence of a topological term. *Phys. Rept.*, 470:93–150, 2009, 0803.1593.
- [62] C. Rohrhofer, Y. Aoki, G. Cossu, H. Fukaya, C. Gattringer, L. Ya. Glozman, S. Hashimoto, C. B. Lang, and S. Prelovsek. Symmetries of spatial meson correlators in high temperature QCD. *Phys. Rev. D*, 100(1):014502, 2019, 1902.03191.
- [63] Andrei Alexandru and Ivan Horváth. Possible New Phase of Thermal QCD. *Phys. Rev. D*, 100(9):094507, 2019, 1906.08047.
- [64] Marco Cardinali, Massimo D’Elia, and Andrea Pasqui. Thermal monopole condensation in QCD with physical quark masses. 7 2021, 2107.02745.
- [65] Andrey Yu. Kotov, Maria Paola Lombardo, and Anton Trunin. Work in progress.